Modeling the Carbon Footprint of Battery-Powered IoT Sensor Nodes for Environmental-Monitoring Applications

Pol Maistriaux, Thibault Pirson, Maxime Schramme, Jérôme Louveaux and David Bol
ICTEAM, UCLouvain, Belgium
{pol.maistriaux,thibault.pirson,maxime.schramme,jerome.louveaux,david.bol}@uclouvain.be

ABSTRACT

The Internet-of-Things (IoT) is frequently presented as an effective tool to monitor our environment and subsequently reduce the environmental footprint of human activities. However, the environmental footprint of IoT nodes themselves is often overlooked. The standardized life-cycle assessment (LCA) methodology can help in this respect. While production impacts can be estimated using LCA databases, use phase impacts are complex to model for battery-powered IoT nodes, commonly used in environmental monitoring. Indeed, battery maintenance operations involve component replacement, transportation and depend on the service lifetime which is strongly influenced by the use phase scenario. We therefore propose a comprehensive open-source parametric model of battery-powered IoT nodes use phase in environmental monitoring applications. The model assesses the overall environmental footprint, including deployment and maintenance, with an enhanced service lifetime evaluation. Using a custom node prototype, additionally validating the underlying power consumption modeling, we then analyze a case study. The use phase model fosters eco-design by allowing the optimal battery capacity identification and highlighting the impact of various parameters on the carbon footprint, e.g., use phase scenario, operating conditions, node positioning, transport scheme, and replacement strategy. Finally, the model can easily be transposed to evaluate economic aspects, motivating the environmental and economic co-optimization.

CCS CONCEPTS

• **Hardware → Impact on the environment**; **Power estimation and optimization**; **Wireless integrated network sensors**.

KEYWORDS

Carbon footprint, IoT sensor node, power consumption, LoRa

ACM Reference Format:
Pol Maistriaux, Thibault Pirson, Maxime Schramme, Jérôme Louveaux and David Bol. 2022. Modeling the Carbon Footprint of Battery-Powered IoT Sensor Nodes for Environmental-Monitoring Applications. In *Proceedings of the 12th International Conference on the Internet of Things (IoT '22), November 7–10, 2022, Delft, Netherlands.* ACM, New York, NY, USA, 8 pages. https://doi.org/10.1145/3567445.3567448

IoT '22, November 7–10, 2022, Delft, Netherlands

ACM ISBN 978-1-4503-9665-3/22/11…$15.00
https://doi.org/10.1145/3567445.3567448

1 INTRODUCTION

The Internet-of-Things (IoT) is rapidly gaining momentum in both research and industry, illustrated by an ever increasing number of connected devices reaching between 12 and 50 billion devices in 2022 [21]. This supports the continuous collection of information in many applicative fields with, e.g., wireless sensor networks (WSNs) to monitor space and things [11] , including ecosystems, cities, homes, and production lines. This explains why IoT is often presented as a powerful way to improve the efficiency of our societies, with high expectations regarding its potential to decrease energy and resource consumption. Yet, deploying such an infrastructure also comes with an environmental burden in terms of energy, water, resource consumption, carbon emissions, and e-waste generation [15, 21]. We are currently confronted with increasing environmental constraints and the need to drastically reduce our greenhouse gas (GHG) emissions, to alleviate our pressure on the environment. Therefore, it is urgent to question the overall efficiency of new technological solutions and to evaluate their environmental footprint ahead of their deployment, a practice which is far from being common today. A life-cycle assessment (LCA) can help in this matter as it is a standardized methodology supporting the evaluation of the environmental impacts over multiple indicators. It considers the full life cycle of a product or device from its production to its use and its end-of-life (EoL). Nevertheless, LCA for IoT is still in its infancy and previous results are scarce [21].

In this work, we provide an LCA-based methodology for modeling the carbon footprint of battery-powered IoT sensor nodes for remote monitoring applications. We propose a parametric bottom-up power consumption model including battery self-discharge caused by leakage to enhance service lifetime estimation. This allows to properly model the use phase and account for impacts of production, deployment and maintenance of the IoT node within a larger infrastructure depicted in Figure 1(a). The contribution of this work lies in the combination of a comprehensive parametric use phase model with the evaluation of production impacts to assess the environmental footprint over the whole life-cycle. The proposed model is available on *GitHub*[1] to stimulate engineers to ecodesign IoT WSNs for low carbon footprint. It is illustrated by a forest monitoring case study, supported by a custom node prototype.

This paper is structured as follows. First, Section 2 provides an overview of previous studies on IoT infrastructures for environmental monitoring. Section 3 details to which extent the environmental footprint of IoT infrastructures is discussed in the literature. Then, the methodology and the models proposed for the carbon footprint evaluation are presented in Section 4. In Section 5, we illustrate this on a case study, assessing the impact of key design parameters. We then discuss economic perspectives in Section 6 before concluding.

[1] https://github.com/PolMaistriaux/IoT_Node_Modeling

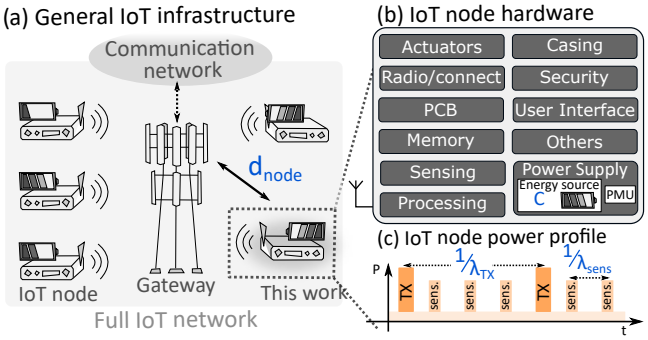

Figure 1: (a) IoT infrastructure and key parameters for environmental monitoring applications. (b) IoT node modules adapted from [21], including the energy storage and power management unit (PMU). (c) Generic IoT node power profile.

2 OVERVIEW OF WSN INFRASTRUCTURE FOR ENVIRONMENTAL MONITORING

Performing an LCA on an IoT sensor node for an environmental-monitoring application requires to identify the key parameters of its use phase. To do so, this section provides an overview of IoT WSN infrastructures for remote environmental monitoring.

The use of IoT nodes as an infrastructure to support environmental monitoring applications is outlined in a growing number of works. For instance, the authors of [26] monitor the temperature, the humidity, and CO_2 concentration in the surroundings, while the authors of [5] developed an urban sound monitoring platform. Similarly, a complete network architecture based on IoT nodes was proposed in [22] to provide precision agriculture and ecological monitoring. Recently, forest fire detection has gained interest and several studies present complete WSN solutions [14, 19].

As we will integrate the use phase in our model, prior power consumption and service lifetime estimations are required. In the above studies, we identify four key parameters of IoT sensor infrastructures impacting those estimations, i.e., (1) the sensing rate λ_{sens} of the monitored environmental parameters, (2) the rate λ_{TX}, either deterministic or probabilistic, at which messages are sent to the network gateway or base station, expressed in messages per day, (3) the battery capacity C, expressed in mAh, and (4) the distance between the node and the base station d_{node}. The topology of the network (star vs. mesh), the communication protocol, the number of nodes and the communication strategy (polling or broadcasting) can vary considerably from one application to the other but these four basic parameters already capture important features of an IoT WSN infrastructure, as illustrated in Figure 1(a). Its building block, the IoT node, can be seen as an electronic device embedding several modules, each one having a specific functionality, as shown in Figure 1(b). This defined hardware used to run determined tasks leads to a specific power consumption profile, as shown in Figure 1(c).

3 PREVIOUS WORK

This sections aims at understanding to which extent the environmental footprint of IoT infrastructures themselves are considered in the scientific literature. Regarding the environmental footprint, it is clear that minimizing the power consumption of the IoT node for a given application is one of the conventional objectives for IoT designers [28]. This minimization extends the node service lifetime, which is beneficial from both economic and environmental perspectives. Power and lifetime are thus key aspects discussed at the node level with detailed development [29] and extensive guidelines on their effective design[6]. In addition, theoretical framework have already been developed to model the power consumption of IoT nodes [18] but while power consumption is modeled in details, power supply non-idealities are overlooked. This yield to an optimistic estimation of the service lifetime. At the network level, both WSN design framework [16] and communication network analysis [27] already consider power and lifetime as key metrics.

Nevertheless, several studies of battery-powered electronic devices showed that environmental hotspots can be found outside the use phase [3, 10]. For instance, [24] shows that minimizing energy consumption or environmental footprint leads to different LPWANs architectures. Indeed, electronic components can exhibit low-power characteristics while embodying a consequent environmental burden from their production. Although they are scarce, some studies attempt to consider the environmental footprint of IoT node production [12, 17, 21, 23] but they neither capture the environmental footprint of the whole IoT infrastructure nor its use phase including maintenance. These aspects are however considered in two of the most comprehensive studies regarding the life-cycle modeling of WSN, namely [2] and [3]. By providing an integrated methodology for the environmental assessment and eco-design of WSN, they pave the way for the present work. Nevertheless, reusability is very limited and few details are provided regarding the modeling.

In this study, we build on previous works modeling the power consumption of IoT nodes to estimate their service lifetime. Moreover, we consider the environmental footprint of IoT node production. This allows to carry the assessment up to the deployment and maintenance of the IoT sensor nodes.

4 METHODOLOGY AND MODEL

In this section, we show how we leverage the general standardized LCA methodology [13] to model the carbon footprint of battery-powered IoT nodes over their life cycle, as detailed in Figure 2(a), by a three steps process. First, we estimate the node service lifetime which defines the maintenance operation rate. We thus propose an in-depth parametric power consumption model. Then, we use state-of-the-art LCA databases to estimate the embodied impacts due to the production of IoT nodes. Finally, the overall carbon footprint is obtained by taking into account the carbon footprint generated by the maintenance operations needed to ensure the proper monitoring over a defined period $T_{monitor}$. Energy harvesting, theoretically alleviating the replacement of batteries, is not considered here for the sake of conciseness. Nevertheless, this methodology could be extended to include it, as well as random failures of the IoT node.

4.1 Service lifetime model

To accurately estimate the service lifetime of a battery-powered node, we first need to properly model its power consumption. The node performs a number of tasks N_{task}, each at a specific rate λ_i, e.g., packet transmission once per hour or sensor measurements every five minutes. Based on the modeling described in several works [18, 20], the energy E_{sys} consumed by the node over a time

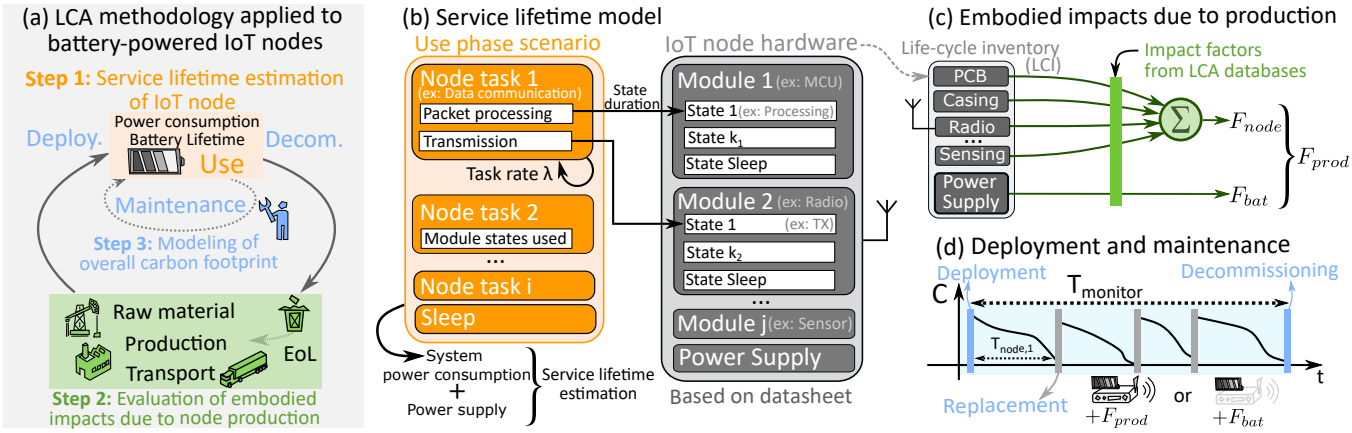

Figure 2: (a) General LCA methodology applied to battery-powered IoT nodes (b) Proposed service lifetime model. (c) Estimation of the embodied environmental impacts due to the node production.(d) Schematic modeling of the node maintenance.

T is the sum of the energy of each task $E_{task,i}$. This is described in Eq. 1 where E_{sleep} is the energy in sleep mode. P_i and T_i respectively refer to the power consumption and duration of each task.

$$\begin{aligned} E_{sys}(T) &= \sum_{i=1}^{N_{task}} \lambda_i E_{task,i} \quad + E_{sleep} \\ &= \sum_{i=1}^{N_{task}} \lambda_i P_i T_i \quad + P_{sleep}\left(T - \sum_{i=1}^{N_{task}} \lambda_i T_i\right) \end{aligned} \tag{1}$$

A task involves one or multiple modules operating in specific states, e.g., communication with a base station involving packet processing by a microcontroller (MCU) and transmission by a radio. This is depicted in Figure 2(b) and expressed in Eq. 2 where N_{mod} is the number of modules within the system and $N_{state,j}$ is the number of states of a given module. E_{sys} linearly depends on the task rates, highlighting the importance of knowing a priori the use phase scenario of the sensor node. For each state, its power consumption $P_{(j,k)}$ and its duration $T_{(i,j,k)}$ for a given task can be found in modules datasheet or by their characterization.

$$E_{sys}(T) = \sum_{i=1}^{N_{task}} \lambda_i \left(\sum_{j=1}^{N_{mod}} \sum_{k=1}^{N_{state,j}} P_{(j,k)} T_{(i,j,k)} \right) + E_{sleep} \tag{2}$$

The power consumption as presented above is agnostic to the power supply scheme. Power management units (PMUs) and energy storage implications must be considered to obtain a relevant estimation of the node service lifetime. Several types of PMU exist but each suffers from inherent conversion losses. We consider here a low-dropout linear regulator (LDO). It converts the energy storage voltage to the one of the modules supplied. The current is however equal on both sides. Thus, the energy drawn from the energy storage, here a battery, is independent of the voltage of the modules. In this case, we can just express E_{sys} in milliampere hour (mAh) by replacing the power consumption terms in Eq. 2 by the current consumption of the modules. An additional current I_q is consumed to power the LDO internal components. The current drawn from the battery is therefore $I_{sys}+I_q$ with $I_{sys} = \frac{E_{sys}(T)}{T}$ the average current consumption. Interestingly, the energy of a battery is often characterized independently of its output voltages, using its capacity C expressed in mAh. The node service lifetime T_{life} is therefore simply the ratio of C and the current drawn from the battery. However, multiple factors limit the service lifetime and add complexity to the model: battery self-discharge, nonlinear battery discharge, and parameters dependency to operating conditions, i.e., temperature and humidity [6]. In this work, only the self-discharge rate of the battery R_{sd} is considered and modeled as a constant discharge per year relative to the initial battery capacity [8]. IoT nodes with high power consumption will have lower theoretical lifetime and therefore suffer less from the self-discharge of their batteries. Finally, Eq. 3 yields the service lifetime of the IoT node.

$$T_{life} = \frac{C}{CR_{sd} + I_q + I_{sys}} \tag{3}$$

4.2 Embodied environmental impacts due to node production

The environmental impacts generated before and after the use phase are important to evaluate as they can represent an important share of the impacts, especially for battery-powered IoT devices [3, 10, 21]. Taking these impacts into account is not straightforward and it can require time and expertise. Yet, a streamlined assessment can also be used, as proposed in [21] for the carbon footprint of IoT nodes. In both cases, the identification of the hardware components is needed: a bill-of-material (BoM) can serve as life-cycle inventory (LCI) which is then used to carry out the evaluation. This is represented schematically in Figure 2(c). Throughout this work, we refer to F as the environmental footprint. We define F_{bat} and F_{node} as the embodied environmental footprint of the production of respectively the battery and of the node (without the battery). F_{bat} can be expressed by its capacity C, and by F_C, the environmental footprint per mAh, which is technology dependent.

$$F_{prod} = F_{node} + F_{bat} = F_{node} + CF_C \tag{4}$$

4.3 Deployment and maintenance

In this study, we focus on the carbon footprint of the sensor node over the monitoring duration. It is important to acknowledge that

the node itself might be replaced at some time, as its lifetime T_{life} can be shorter than the monitoring duration $T_{monitor}$. This leads to maintenance operations whose carbon footprint and frequency must be taken into account, as shown in Figure 2(d).

Several information are thus required. First, the replacement strategy defines whether only the battery or the complete node is replaced. The former minimizes the carbon footprint at the production level. The second is more robust against node wear-out due to degradation of the casing or electronic component aging as well as against technical obsolescence. This yields the replacement carbon footprint F_{rep}. Second, the sensor nodes transportation specifies the distance d_{trans} to and from the monitoring site, the distance traveled on the site, as well as the type of vehicle used. The resulting transportation footprint is divided among the nodes carried in the vehicle, yielding F_{trans} the transportation footprint per node. This theoretical analysis considers an equal value of F_{trans} for deployment, decommissioning and maintenance. Finally, Eq. 5 expresses the overall carbon footprint $F_{T_{monitor}}$. It can be normalized per monitoring year as $F_T = \frac{F_{T_{monitor}}}{T_{monitor}}$ to obtain a yearly footprint.

$$F_{T_{monitor}} = \underbrace{[F_{prod} + 2 \times F_{trans}]}_{\substack{\text{Deployment and} \\ \text{decommissioning}}} + \underbrace{[F_{rep} + F_{trans}]}_{\text{Maintenance}} \underbrace{\left(\frac{T_{monitor}}{T_{life}} - 1 \right)}_{\substack{\text{Number of} \\ \text{Maintenance}}}$$
$$\text{where } F_{rep} = \begin{cases} F_{prod} & \text{if complete node replacement} \\ F_{bat} & \text{if only battery replacement} \end{cases} \tag{5}$$

To go forward, we make two hypotheses. First, we work with a fixed battery cell, meaning F_C and C are fixed. The node battery capacity is thus increased by connecting N_{bat} cells in parallel, leading to an overall battery capacity of $N_{bat}C$. The battery technology selection is dependent on the target application, some having harsher operating conditions. Second, for the sake of conciseness, complete node replacement is assumed although battery replacement results can be derived easily. Using Eqs. 3 and 5, we obtain:

$$\begin{aligned} F_T &= \left[F_{prod} + F_{trans}\right] \frac{1}{T_{life}} + \underbrace{F_{trans}}_{\text{Decom.}} \\ &= \left[F_{node} + \underbrace{N_{bat} C F_C}_{F_{bat}} + F_{trans} \right] \left(\frac{N_{bat} C R_{sd} + I_{sys} + I_q}{N_{bat} C} \right) + F_{trans} \\ &= \left[F_{node} + F_{trans}\right] R_{sd} + N_{bat} C F_C R_{sd} \\ &\quad + \frac{\left[F_{node} + F_{trans}\right] \left(I_{sys} + I_q\right)}{N_{bat} C} + F_C \left(I_{sys} + I_q\right) + F_{trans} \end{aligned} \tag{6}$$

Eq. 6 points out several implications. First, we see that the expression linearly depends on the system current consumption I_{sys} and therefore on the tasks rates λ_i, but also on the self-discharge rate R_{sd}, and on the transportation footprint F_{trans}. Regarding the battery capacity $N_{bat}C$, it shows a trade-off. Using large battery capacity increases the node lifetime, reducing the number of maintenance. This is highlighted by the $1/N_{bat}C$ dependency in the third term. However, employing lower battery capacities limits the energy wasted by the total self-discharge due to the parallel connections between battery cells. This is shown by the linear dependency of F_T with $N_{bat}C$ in the second term. Therefore, there is an optimal battery capacity minimizing the carbon footprint, depending on the self-discharge rate, and therefore the operating conditions, on the task rates, and on the transportation characteristics.

5 CASE STUDY: FOREST MONITORING

In this section, we apply the proposed methodology to a forest monitoring case study to highlight its use as an eco-design tool. It is supported by a custom node prototype which we first characterize and use to validate the power consumption model. We then evaluate the embodied carbon footprint of the prototype and analyze the impact of multiple parameters on the power consumption, the service lifetime and the overall environmental footprint.

5.1 Context

We focus on the monitoring of forest via the sensing of temperature (T), humidity (H), pressure (P) and gas concentration (G). The sensor node processes the environmental parameters and computes the fire weather index (FWI). It is a fire risk indicator developed by the Canadian Forest Service (CFS) whose relevance in WSN has already been studied [14, 19]. As forest monitoring does not ensure the presence of a base station near the sensor location, low-power wide area network (LPWAN) technologies are relevant to ensure communication capabilities at long range and for highly-attenuated propagation path. Among LPWANs, LoRa is a standard physical layer built around a narrow band chirp-spread spectrum modulation [27]. The modulation is property of *Semtech* but point-to-point communication can be freely established using *Semtech*'s devices, e.g., the common SX1276 using the 868 MHz ISM frequency band.

5.2 Prototype and characterization

In this prototype, the temperature, humidity, pressure, and gas concentration measurements are averaged up to the LoRa transmission time. A simplified version of the FWI is then computed and transmitted. The main goal of this prototype is to validate the power consumption model of Section 4.1. The PMU and energy storage were not included in the prototype even though they were selected to estimate its lifetime and environmental footprint. The structure as well as a photograph of the prototype are shown in Figure 3 and details about its modules are provided below.

5.2.1 MCU: Apollo3 Blue. The Apollo3 Blue is an ultra-low power MCU developed by *Ambiq* targetting baterry-powered devices [1] with a sleep and active current of respectively 3.2μA and 10.3μA/MHz at 3.3V. To ease development and power measurement, an evaluation board (EVB) from *Ambiq* has been used.

5.2.2 Sensor: BME680. Developed by *Bosch*, the BME680 sensor embeds T, P, H, and G measurements [4]. Its ultra-low power mode imposes the sensing period to five minutes for an average current of 90μA. The digital readings ease the interfacing with the MCU via an I^2C connection. An evaluation board has also been used.

5.2.3 Radio module: RFM95. The SX1276 from *Semtech* enables long range communication with a receiver sensitivity down to -148 dBm and a transmit power of maximum 20 dBm [25]. Including the

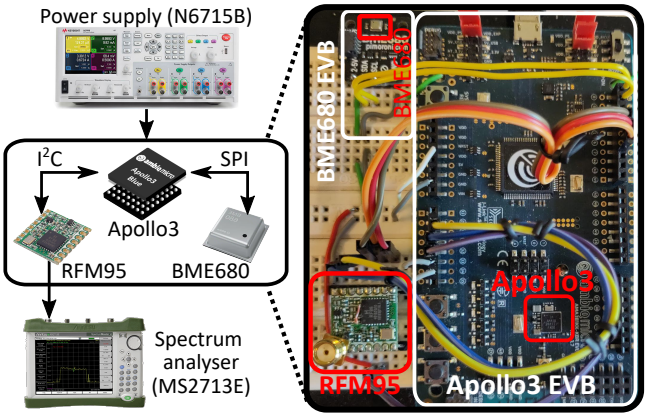

Figure 3: Schematic view of the prototype and of the characterization setup. Prototype photograph is depicted.

	Module state	Measure	Datasheet	Characterization
MCU	Sleep	I_{sleep}	3.2 μA	2.7 μA
	Active @48MHz	I_{active}	494 μA	573 μA
	SPI	T_{SPI}	- ms	306 ms
	I^2C	T_{I^2C}	- ms	106 ms
	FWI calc.	T_{FWI}	- ms	1.5 ms
Sensor	Sleep	I_{sleep}	0.15 μA	32.8† μA
	TPHG ††	I_{TPHG}	90 μA	78.2 μA
Radio	Sleep	I_{sleep}	0.2 μ A	0.6 μA
	RX	I_{RX}	11.5 mA	11.3 mA
	TX @+17dBm	I_{TX}	87 mA	86.23 mA
	TX @+20dBm	I_{TX}	120 mA	119.05 mA

† BME680 EVB sleep power significantly differs from BME680 datasheet. Characterization value was therefore used to validate the power consumption model.
†† Average current when sensor measurements are performed at 5 minutes interval.

Table 1: Operating electrical characteristics of the three modules of the prototype, i.e. Apollo3 Blue, RFM95 and BME680, from datasheet and characterisation at 3.3V

SX1276 chip, the RFM95 interfaces this module with the required components, i.e., crystal oscillator, antenna matching networks, and RF switches, requiring only a *SPI* communication with the MCU.

5.2.4 PMU: XC6206. The LDO voltage regulator XC6206 from *Torex* has been selected for its low current consumption of typically 1μA.

5.2.5 Energy storage: Alkaline AA batteries. Those batteries were selected due to their omnipresence in battery-powered devices, their low cost and their low self-discharge rate [6]. They reach a standard battery capacity of 2800 mAh. Moreover, rechargeable batteries were not considered due to their lower energy density and operating temperature. In order to obtain the 3.3V required to supply the sensor node, three AA batteries are connected in series, forming a single battery module of 4.5V. Parallel connections between battery modules increase the overall battery capacity.

To characterize the prototype, a source measure unit (SMU) has been used to supply the modules and capture their current consumption. Energy of each state can be derived from the measurements of both the current and the duration of the state. A spectrum analyzer connected via an SMA cable to the RFM95 measures the transmitted power to verify datasheet values experimentally. The setup is represented in Figure 3 and results are provided in Table 1.

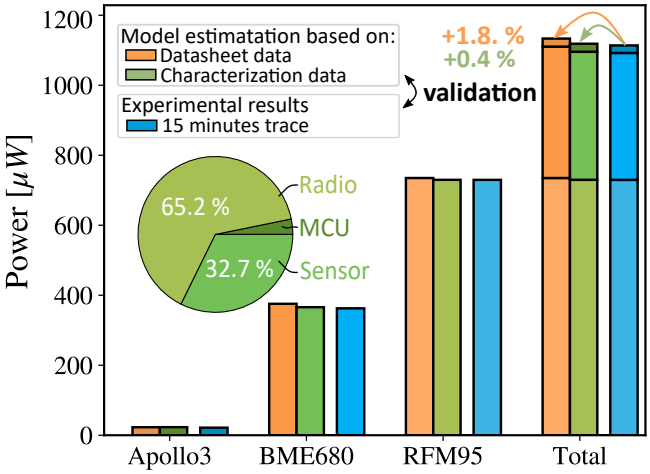

Figure 4: Validation of the power consumption model based on the prototype for λ_{sens} = 5 minutes, λ_{TX} = 15 minutes and the following LoRa communication parameters: 50 bytes payload, SF12 and P_{TX} at 17dBm.

5.3 Power consumption model validation

In order to validate the power consumption model presented in Section 4.1, we used it to estimate the power consumption of a defined use phase scenario. Sensing of T, P, H, and G is performed at five minutes intervals. Their values are averaged over 3 measurements before calculating the FWI. The result is sent as a 50-bytes payload using the spreading factor 12 and a transmit power of 17dBm. Two model estimations were calculated, one using datasheet values when possible and the other using only characterization values.

To validate the model estimations, fifteen minutes current traces were captured for the same use phase scenario, using the setup presented in Figure 3. From those traces, we extracted the average drawn currents. The comparison results are depicted in Figure 4, showing the distribution of the consumed power. Our model gives a proper estimation of the power consumption, with an error of +1.8% and +0.4% using datasheet or characterization values, respectively. The high sleep current of the BME680 is due to external components of its EVB. Since this board is not intended for low power applications, the datasheet value of 0.15μA for the sleep mode of the BME680 is considered for the rest of this work.

5.4 Service lifetime estimation

To show how the model allows for a comprehensive parametric analysis, we first study the power consumption and service lifetime of the node. We consider three key parameters, i.e., the transmission rate λ_{TX}, the node-base station distance d_{node}, and the self-discharge rate R_{sd}. The latter is hard to define and significantly depends on the operating conditions, i.e., the temperature and the humidity. Therefore, R_{sd} higher than those provided in datasheets, e.g., 2 – 3% for alkaline cells, should be tested for precaution.

We first analyze the impact of the node-base station distance d_{node} on the power consumption, as shown in Figure 5. The path loss has been estimated using an ad hoc LoRa forest propagation model [7]. To minimize power consumption at each distance, optimal LoRa parameters are assumed. Here we act first on the transmit power P_{TX} which can be adjusted on the RFM95 in 1dB increments,

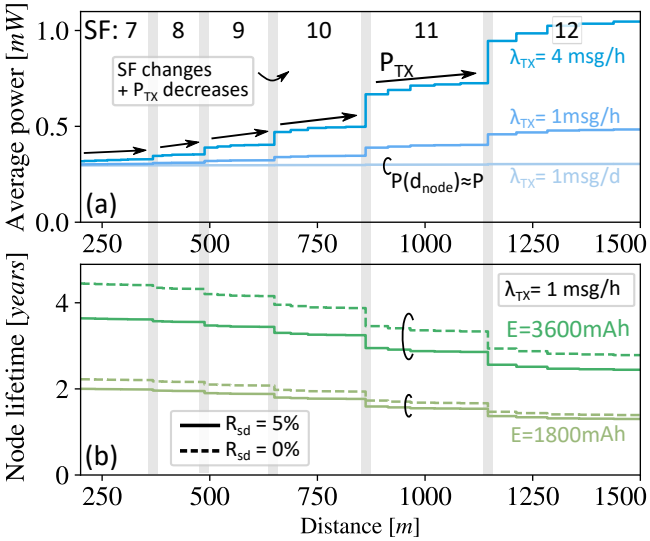

Figure 5: Impact of the node-base station distance on the power and lifetime for (a) different transmission rates, (b) different battery capacities and self-discharge rates.

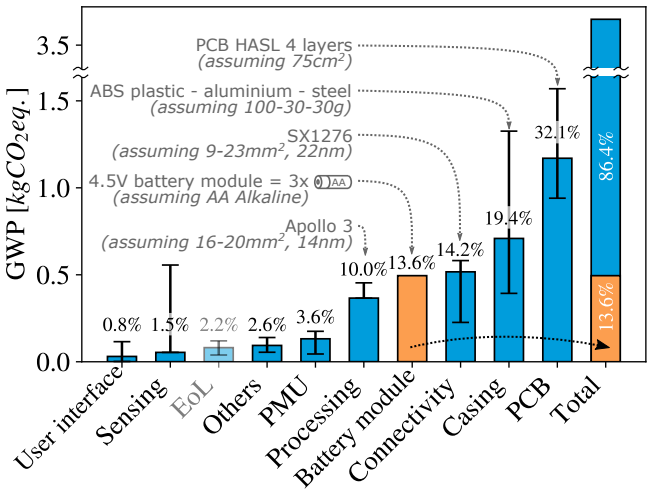

Figure 6: Breakdown of the cradle-to-gate carbon footprint for the prototype. The relative share with respect to the total (3.65 kgCO_2eq) is given for each module.

leading to consumed current steps. Second, we can act on the spreading factor (SF) which takes values from 7 to 12. An increase in SF of one results in twice the transmission time, and therefore twice the energy consumption, as well as a gain in SNR of 2.5 dB. We can see in Figure 5(a) the significant impacts of the SF changes on the power consumption and the smaller steps due to P_{TX} changes.

Moreover, the figure shows the effect of the transmission rate λ_{TX}. Due to the linear dependency of the power consumption on the tasks rates, λ_{TX} variations lead to proportional power changes. This becomes clearer at long distances where the transmissions dominate the power consumption. The sensing frequency could be analyzed but the results exhibit a similar dependency as for λ_{TX}. In Figure 5(b), communication distance appears to be a determining factor regarding the node service lifetime, highlighting the importance of proper node positioning. Finally, the self-discharge rate impact increases with the node ideal lifetime, as expected.

5.5 Embodied carbon footprint due to node production

In order to evaluate the carbon footprint related to the production of the prototype, we used the GaBi professional and GaBi Extension XI (Electronics) databases. These are commercial state-of-the-art LCA databases allowing a specific modeling of the different electronic components. As this study focus only on the carbon footprint, the global warming potential (GWP) was modeled with the LCA software GaBi using the ReCiPe 2016 midpoint (H) method.

The carbon footprint evaluation is based on an optimized hardware design in order not to introduce a bias as evaluation boards and development prototype are clearly under-optimized for configurability and debugging reasons. Figure 6 shows the breakdown of the carbon footprint for the production of a node, together with details regarding a streamlined LCI for the modules with a significant contribution. The relative share is given for each module, as well as lower and upper bounds for the best and worst cases. This points out that the PCB accounts for about 32% of the overall production carbon footprint, while the casing and the ICs contribute up to 19% and 14%, respectively. The total embodied carbon footprint of the node is about 3.65 kgCO_2eq while the production of a single Alkaline battery module (3 AA cells) is evaluated to 0.49 kgCO_2eq. Therefore, the battery production accounts for about 14% of the total carbon footprint, if a single battery module is used to power the node. The carbon footprint associated with the end-of-life (EoL) is also taken into account although we assumed a basic scenario, i.e., electronics parts end up in an incineration plant and plastic parts in landfill. This should be seen as a lower bound, although the carbon footprint generated during the EoL management is usually not a hotspot for battery-powered devices [9, 21].

5.6 Deployment and maintenance of the nodes

To discuss the overall carbon footprint including deployment and maintenance, detailed information on the monitoring application is required. We assume the monitoring duration $T_{monitor}$ is thirty years, leading to a 2050 perspective. We also make some hypotheses on the transport scheme to show the influence of key parameters. As explained in Section 4.3, we assume the operator travels a distance d_{trans}, expressed in km, to and from the monitoring site, plus 5 km when on site. Moreover, we arbitrarily assume that 100 IoT nodes are carried out at the same time when conducting the deployment and decommissioning, while 10 are assumed for the maintenance.

5.7 Results

Every aspect of the monitoring application being now properly defined, we can focus on the influence of multiple parameters on the carbon footprint. Eq. 6 implies that the yearly carbon footprint F_T depends linearly on multiple parameters of the models, i.e., the transmission frequency λ_{TX}, the sensing frequency λ_{sens}, the self-discharge rate R_{sd}, and the transportation footprint F_{trans}. As shown in Figure 7 for λ_{TX}, low values of those parameters have thus negligible impacts on the environmental footprint due to the initial non-zero carbon footprint, or GWP. For instance,

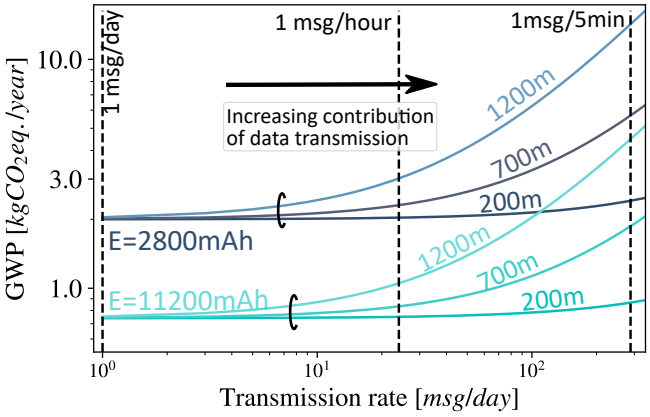

Figure 7: Impact of transmission rate, node-base station distance and battery capacity on the carbon footprint.

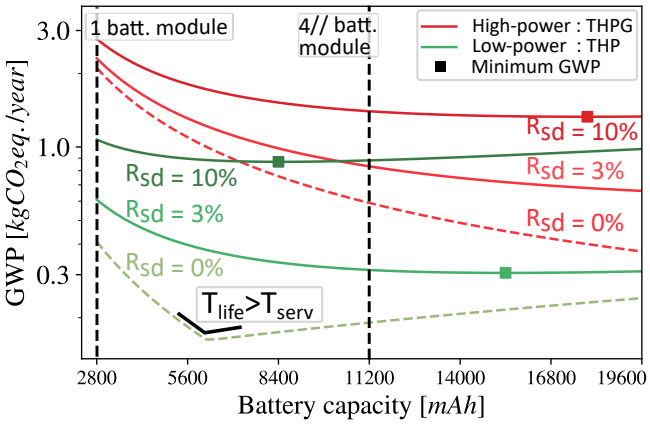

Figure 8: GWP with respect to battery capacity for two types of sensing : T, P and H with or without G. Self-discharge rates R_{sd} of 0, 3 and 10% are considered. The node-base station distance is 700 m and one packet is sent per hour.

sensing and self-discharge still induce maintenance even if there is no transmission. However, those parameters can rapidly become non-negligible as observed in the figure. Depending on the node-base station distance, the point at which transmissions become dominant on the environmental footprint significantly differs.

As discussed in Section 4.3, F_T exhibits an optimal choice of battery capacity. It strongly depends on the self-discharge rate, as well as on the node power consumption. To illustrate this, Figure 8 compares the sensing of T, P and, H with and without G. The latter drastically reduces the BME680 average power from 90μA to 3.7μA [4]. Moreover, ideal, standard, and pessimistic R_{sd} are analyzed. The minimum of the different curves are pointed out, highlighting that lower power applications should embed smaller batteries. The additional lifetime enabled by a higher battery capacity is partially lost to self-discharge. Discontinuities in the function are caused by the oversizing of the battery. Indeed, this happens when the node reaches a service lifetime superior to the one of its application and the remaining battery capacity becomes prohibitive.

The transportation footprint F_{trans} due to deployment, maintenance and decommissioning, can strongly vary based on the site

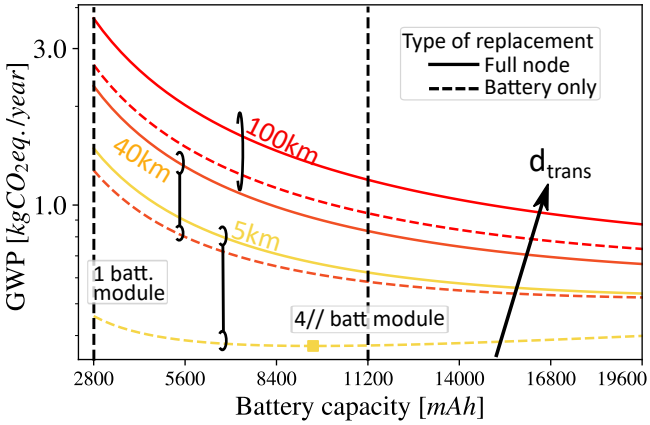

Figure 9: GWP with respect to battery capacity for transport distances of 5, 40 and 100 km. Full-node replacement and battery-only replacement strategies are depicted. The node-base station distance is 700 m and one packet is sent per hour.

localisation, the transportation type, or the number of nodes carried. This also affect the overall footprint F_T, as shown in Figure 9 where different traveled distances d_{trans} and replacement strategies are evaluated. It can be observed that low values of d_{trans} tend to make the impact of different replacement strategies non-negligible, battery replacement becoming much more efficient.

This analysis highlights the use of the model to identify hotspots, which have a significant impact on the environmental footprint of the IoT node, and change depending on the numerous design and use phase parameters. For example, the impact of transmissions drastically increases for long communication distances and high transmission rates, while an highly effective transport scheme tends to make the transportation footprint per node negligible.

6 ECONOMIC PERSPECTIVES

As the carbon footprint cannot capture all environmental impacts, the model proposed in this study is built to ease its transposition to other indicators. For instance, it would be of interest to consider environmental indicators such as energy, water, or eco-toxicity. Similarly, the underlying model can also be used to evaluate economic aspects of the IoT infrastructure by using the financial cost instead of the environmental footprint in Eqs. 4, 5, and 6. For a given hardware of the IoT node and thus fixed production impacts, dependencies on the discussed parameters vary. Even though linear trends hold for both economic and environmental perspectives, battery capacity will exhibit a different optimum for both aspects. The co-modeling of environmental and economic impacts is critical today for two key reasons. First, it can point out the arbitration needed between environmental and economic perspectives, as eco-design decisions can impact both aspects similarly or in opposite directions. This can also help evaluating the cost of such an infrastructure to define new business models for IoT providers. Second, it can support the evaluation of important supply chain modifications on both perspectives. For instance, relocating manufacturing in Europe as opposed to Asia and/or the recent supply chain shortage of chips lead to a strong increase in the price of electronic components. Future works will analyzed this into more details.

7 CONCLUSION

In this work, we implemented a complete LCA-based methodology for the parametric analysis of IoT nodes in the context of environmental monitoring, often involving harsh operating conditions and remote areas. We modeled the environmental footprint of battery-powered IoT sensor nodes over the monitoring duration, considering deployment and maintenance. An in-depth evaluation of the node service lifetime was proposed, including power supply non-idealities such as the battery self-discharge. It was combined with an evaluation of its production footprint using state-of-the-art LCA databases. The proposed model was applied to a forest monitoring node prototype, also validating the underlying power consumption model with an error below 1.8%.

A parametric analysis of the power consumption, the service lifetime and the overall carbon footprint was then conducted based on several key yet sometimes overlooked parameters. The proposed model helps to assess the impact of the numerous parameters in various scenarios. Indeed, it is made easy to select coherent tasks rates, to search for battery capacity optimum or to evaluate the impact of different transport schemes, replacement strategies, operating conditions, and node positioning. This highlights the model capability to identify hotspots, both in the design and in the use phase. This is illustrated by data transmissions, rapidly becoming the main driver of maintenance operations when the transmission rate and the communication distance increase. The model thus points out where optimizations should be conducted first in the design, deployment and maintenance of the IoT sensor nodes. To further encourage eco-design practices, the proposed model is available on *GitHub*[2].

Finally, the model can easily be transposed to other indicators, e.g., economic aspects by using financial prices instead of environmental footprints. Future works should investigate the environmental and economic impacts co-optimization.

1. What are the three main aspects considered in the LCA methodology for modeling the carbon footprint of battery-powered IoT nodes?
Service lifetime estimation, production impacts, and maintenance impacts.

2. How does the model account for the energy consumption of the different modules in the IoT node?
Through calculations based on specific tasks, their frequency, and operational data for each module, such as MCU, sensors, and radio.

3. Why is the environmental impact of node production considered important in the paper, and how does it differ from the impact during the use phase?
The production impact includes the burden of materials and manufacturing, which can outweigh the energy consumption during use, especially for low-power nodes.

4. What limitations of the model are discussed by the authors, and what potential extensions do they propose?
Limitations include the absence of energy harvesting technologies and random failures; proposed extensions involve modeling these variables.

5. How could the paper's findings influence eco-sustainable design for IoT systems?
The findings can guide design choices to optimize service lifetime, reduce maintenance needs, and select components with minimal overall environmental impact.

ACKNOWLEDGMENTS

This work was supported by the FRS-FNRS through a FRIA grant. It was also supported by the FEDER and the Wallonia within the Wallonie-2020.EU program.

REFERENCES

[1] Ambiq. 2022. *Apollo3 Blue MCU - Datasheet.* Technical Report.
[2] Jérémy Bonvoisin, Alan Lelah, Fabrice Mathieux, and Daniel Brissaud. 2012. An environmental assessment method for wireless sensor networks. *Journal of Cleaner Production* 33 (2012), 145–154.
[3] Jeremy Bonvoisin, Alan Lelah, Fabrice Mathieux, and Daniel Brissaud. 2014. An integrated method for environmental assessment and ecodesign of ICT-based optimization services. *Journal of Cleaner Production* 68 (2014), 144–154. https://doi.org/10.1016/j.jclepro.2014.01.003.
[4] Bosch. 2022. *BME680 - Low Power Gas, Pressure, Temperature & Humidity - Datasheet.* Technical Report.
[5] Chesney Buyle, Bart Thoen, Bert Cox, Matthias Alleman, Stijn Wielandt, and Lieven De Strycker. 2019. Ultra-Low-Power Smart Sensing Platform for Urban Sound Event Monitoring. *Proceedings of the 2019 Symposium on Information Theory and Signal Processing in the Benelux*, 35–40. http://www.w-i-c.org/
[6] Gilles Callebaut, Guus Leenders, Jarne Van Mulders, Geoffrey Ottoy, Lieven De Strycker, and Liesbet Van der Perre. 2021. The Art of Designing Remote IoT Devices—Technologies and Strategies for a Long Battery Life. *Sensors* 21, 3 (Jan. 2021), 913. https://doi.org/10.3390/s21030913
[7] Gilles Callebaut and Liesbet Van der Perre. 2020. Characterization of LoRa Point-to-Point Path Loss: Measurement Campaigns and Modeling Considering Censored Data. *IEEE Internet of Things Journal* 7, 3 (March 2020), 1910–1918. https://doi.org/10.1109/JIOT.2019.2953804
[23] Ernesto Quisbert-Trujillo, Thomas Ernst, Karine Evrard Samuel, Emmanuel and Elise Monnier. 2020. Lifecycle Modeling for the Eco Design of the Internet of Things. *Procedia CIRP* 90 (Jan. 2020), 97–101. https://doi.org/10.1016/j.procir.2020.02.120
[24] Mina Rady, Jean-Philippe Georges, and Francis Lepage. 2021. Can Energy Optimization Lead to Economic and Environmental Waste in LPWAN Architectures? *ETRI Journal* 43, 2 (2021), 173–183. https://doi.org/10.4218/etrij.2019-0524
[25] Semtech. 2020. *SX1276/77/78 - 137-1050 MHz Ultra Low Power Long Range Transceiver - Datasheet.* Technical Report.
[26] Jalpa Shah and Biswajit Mishra. 2016. IoT Enabled Environmental Monitoring System for Smart Cities. In *2016 International Conference on Internet of Things and Applications (IOTA)*. 383–388. https://doi.org/10.1109/IOTA.2016.7562757
[27] Ritesh Kumar Singh, Priyesh Pappinisseri Puluckul, Rafael Berkvens, and Maarten Weyn. 2020. Energy Consumption Analysis of LPWAN Technologies and Lifetime Estimation for IoT Application. *Sensors* 20, 17 (Aug. 2020), 4794. https://doi.org/10.3390/s20174794
[28] Jesús Martín Talavera, Luis Eduardo Tobón, Jairo Alejandro Gómez, María Alejandra Culman, Juan Manuel Aranda, Diana Teresa Parra, Luis Alfredo Quiroz, Adolfo Hoyos, and Luis Ernesto Garreta. 2017. Review of IoT Applications in Agro-Industrial and Environmental Fields. *Computers and Electronics in Agriculture* 142 (Nov. 2017), 283–297. https://doi.org/10.1016/j.compag.2017.09.015
[29] Bart Thoen, Gilles Callebaut, Guus Leenders, and Stijn Wielandt. 2019. A Deployable LPWAN Platform for Low-Cost and Energy-Constrained IoT Applications. *Sensors* 19, 3 (2019). https://doi.org/10.3390/s19030585

[2]https://github.com/PolMaistriaux/IoT_Node_Modeling